Response to Reviewer 1 comments for manuscript ID egusphere-2024-175. The comments are given in an italic typeface, and the responses are given in a bold typeface. The corresponding changes in the revised manuscript are highlighted in red.

1.1) Review: Dimethyl sulfide (DMS) climatologies, fluxes, and trends - Part B: Sea air fluxes By Sankirna D. Joge et al. The paper evaluated DMS fluxes based on different DMS climatologies, windspeed fields and gas transfer velocity parameterisations. The paper further evaluates which of those influences is contributing most to the differences in total flux. While the study is generally providing some useful insights, I would recommend some major revisions to the paper. In particular I am missing a proper discussion section, including comparisons to earlier comparisons among k-parameterisations and DMS fluxes. What is new/different here compared to earlier ones, are there new scientific insights/messages? Furthermore, the scale differences (temporal and spatial) need to be better discussed with respect to the in situ vs calculated fluxes. It is questionable that those are comparable in this study. The writing is generally ok, but some English language editing particularly with respect to missing articles is recommended. (I provided annotations in the pdf)

Response: We thank the reviewer for the interest and the thorough review of the manuscript and also for providing the annotations in the article, which have been included in the revised manuscript. The comments given in the pdf have also been answered. Answers to the detailed comments are given one by one in this document.

1.2) ***Detailed comments*** *(smaller notes and language edits are only in the pdf annotations)*

1.2.1) The introduction has generally rather old references and could do with some updates. Especially given the discussions following Quinn and Bates 2011, maybe some newer refs would help to emphasize DMS studies are still valuable.

Response: The introduction section is updated with text (L25 – L40, L42 – L45), and new references have been cited.

1.2.2) L63: is Ca ignored here? Maybe see Steiner and Denman, 2008 (https://doi.org/10.1016/j.dsr.2008.02.010, their Fig 6) on difference in flux if the atmospheric concentration is ignored in higher emission regions, for example station papa (note dependence on boundary layer)

Response: Yes, the reviewer is right that we have ignored the impact of Ca, which can play an important role in determining the total flux. However, considering the fluxes we report here are for chemistry transport models which do not include the impact of Ca, the comparison between the parameterisations is valid. We have clarified this in the revised manuscript (L80 – L83).

1.2.3) Section 2: Please clarify that you are not comparing flux calculations but parameterisations for the gas exchange velocity k (correct throughout). Also please add a k vs u figure and discuss the differences among parameterisations.

Response: This is now explicitly mentioned (L170– L172). The k vs u plots are also added in the supplementary text (Figs. S1 – S7).

1.2.4) Please be accurate with the wording. The word observed should be used for actual observations in the field, not what is seen in a parameterization-derived figure. Please correct throughout as it is confusing.

Response: The changes have been made in the manuscript throughout as per the reviewer's suggestion.

1.2.5) If talking about sensitivity, ensure the sensitivity has been defined and tested, if not use a different word. Similarly, if using the word significant, a significance test needs to be made. If not, please use another word. (Locations indicated in annotated pdf).

Response: Corrected throughout the manuscript.

1.2.6) L186 …seen in the LM86 parameterization, which consistently displays lower values than the N00b parametrization". This is to be expected if linear versus quadratic windspeed dependence is applied – should be discussed in context of a k-u figure.

Response: Yes, the reviewer is right in this surmise. A discussion on why LM86 shows lower values than N00b is now included (L230 – L231).

1.2.7) As a general rule, other than continents or large ocean basins, please identify specific locations in the map, e.g., Mauritius, Somalia... (so the reader doesn't have to take out an atlas to follow the discussion)

Response: The lines about maximum values and their respective location are removed from the text, and a Table S2 has been added in the supplementary text to make it easier to read.

1.2.8) L258 …Overall, the choice of seawater DMS estimation method has larger influence on sea-air DMS flux than the choice of flux parameterization (Bhatti et al., 2023). Is this a result from Bahtti et al or from this study, if the latter clarify that this is also highlighted/shown in Bhatti et al. if it is not a result from this study it should be in the intro or discussion.

Response: The results are from this study, which can also be seen in Fig. 3. The study by Bhatti et al. (2023) is cited to support our result, along with Tesdal et al. (2016) (L281).

1.2.9) A discussion session is missing. While some components of the result section can be moved into the discussion session, I am missing a comparison to earlier parameterisation intercomparisons, especially Tesdal et al 2015, https://doi.org/10.1071/EN14255 , but also e.g., Steiner et al. https://elischolar.library.yale.edu/journal_of_marine_research/170 their Fig 1. Also, some discussion on why and where the parameterisations differ - link to k versus u figure. Improved discussion on spatial and temporal scales in context with the comparison to in situ observations.

Response: A detailed discussion is added in Section 4, and the points suggested by the reviewer are now included in this section (L305 - L342).

1.2.10) Results section and table 1: The text with the long lists of max and mins is rather tedious to read. Maybe remove a good part of it and add a max column into Table 1 or add a table with max/mean/mins in the Appendix, potentially divided into different ocean basins.

Response: As suggested by the reviewer, tables S2 and S3 have been added to the supplementary text, and the detailed description of the results has been removed.

https://doi.org/10.5194/egusphere-2024-175
Preprint. Discussion started: 27 February 2024

Dimethyl sulfide (DMS) climatologies, fluxes, and trends - Part B: Sea-air fluxes

Sankirna D. Joge[1,2], Anoop S. Mahajan[1, *], Shrivardhan Hulswar[1], Christa A. Marandino[3], Martí Galí[4,5], Thomas G. Bell[6], Mingxi Yang[6] and Rafel Simo[4]

[1]Indian Institute of Tropical Meteorology, Pune, India

[2]Savitribai Phule Pune University, Pune, India

[3]Research Division 2-Biogeochemistry, GEOMAR Helmholtz Centre for Ocean Research Kiel, Kiel, Germany

[4]Institut de Ciències del Mar (CSIC), Barcelona, Catalonia, Spain

[5] Barcelona Supercomputing Center (BSC), Barcelona, Spain

[6]Plymouth Marine Laboratory (PML), Plymouth, UK

Correspondence to: Anoop S. Mahajan (anoop@tropmet.res.in)

Abstract. Dimethyl sulfide (DMS) significantly contributes to cloud condensation nuclei (CCN) formation in the marine environment. DMS is ventilated from the ocean to the atmosphere, and in most models, this flux is calculated using seawater DMS concentrations and a sea-air flux parameterization. Here, climatological seawater DMS concentrations from interpolation and parameterization techniques are passed through seven flux parametrizations to estimate the DMS flux. The seasonal means of calculated fluxes are compared to identify differences in absolute values and spatial distribution, which show large differences depending on the flux parameterization used. In situ flux observations were used to validate the estimated fluxes from all seven parameterizations. Even though we see a correlation between the estimated and observed values, all methods underestimate the fluxes in the higher range (>20 µmol m^{-2} d^{-1}) and overestimate the fluxes in the lower range (< 20 µmol m^{-2} d^{-1}). The estimated uncertainty in DMS fluxes is driven by the uncertainty in seawater DMS concentrations in some regions but by the choice of flux parameterization in others. We show that the resultant flux is hence highly sensitive to both and suggest that there needs to be an improvement in the estimation methods of global seawater DMS concentration and sea-air fluxes for accurately modeling the effect of DMS on the atmosphere.

1 Introduction

Dimethyl sulfide (DMS) is a marine-derived compound responsible for influencing climate change, which is obtained from the phytoplankton life cycle through the enzymatic cleavage of dimethylsulfoniopropionate (DMSP) (Andreae and Crutzen, 1997; Charlson et al., 1987; Simó, 2001). The DMS emitted from the surface ocean is responsible for up to 70 % of the natural sulfur emissions into the global atmosphere (Andreae and Raemdonck, 1983; Carpenter et al., 2012). Due to its effect on

https://doi.org/10.5194/egusphere-2024-175
Preprint. Discussion started: 27 February 2024

incoming solar radiation, this biogeochemical cycle plays a vital role in the Earth's climate system (Andreae and Crutzen, 1997; Charlson et al., 1987).

The emission of DMS occurs due to differences in concentrations of DMS in the seawater and the atmosphere. The sea-air gas transfer is a complex process, with the wind proven to be one of the most influencing factors (Jähne et al., 1979). Hence, the sea-air gas transfer is parameterized as a function of wind speed. Kettle and Andreae (2000) carried out a comparative study between three parametrizations viz., Liss & Merlivat (1986), Wanninkhof (1992), and Erickson (1993). They concluded that a significant uncertainty in the flux parameterizations leads to uncertainties in estimating the global DMS flux. Furthermore, different datasets for wind speed, sea surface temperature (SST), and sea surface DMS concentration resulted in relatively small variations in these calculated fluxes (≤ 25 %) (Kettle and Andreae, 2000).

Here, we compare global sea-air DMS fluxes derived using seven different gas transfer velocity parameterizations using wind speed and SST. The comparison is conducted using different seawater DMS estimations to identify whether the uncertainty in the emissions is larger because of the uncertainty in seawater DMS concentrations or the flux parameterization. We use one interpolation-based seawater DMS concentration climatology ((Hulswar et al., 2022), hereafter referred to as H22) and two parameterization-based seawater DMS climatologies (Galí et al. (2018), hereafter referred to as G18 and Wang et al. (2020), hereafter referred to as W20. A comparison between the three seawater DMS climatologies is presented in the sister paper (Joge et al., referred to as Joge: Part A). Here, we inter-compared the DMS fluxes estimated using seven sea-air flux parameterizations and in situ DMS fluxes and identified the drivers of their uncertainties.

2 Data and methodology

For DMS flux calculation, seven parametrization schemes (LM86 (Liss and Merlivat, 1986), E93 (Erickson, 1993), N00a, N00b (Nightingale et al., 2000), Ho06 (Ho et al., 2006), GM12 (Goddijn-Murphy et al., 2012), W14 (Wanninkhof, 2014)) are used with the seawater DMS climatological data of H22, G18, and W20 (please check Joge: Part A for a comparison between the seawater DMS estimations). Each flux parametrization scheme uses wind speed, and some also use SST to estimate the DMS sea-air flux. Wind speed and SST were obtained from the National Centers for Environmental Prediction (NCEP; https://psl.noaa.gov/data/gridded/index.html) (Kalnay et al., 1996) and Centennial in situ Observation-Based Estimates (COBE; https://psl.noaa.gov/data/gridded/data.cobe.html) (Ishii et al., 2005), respectively, for the years from 1948 to 2022, and then monthly averaged to calculate the fluxes.

In general, all the parameterizations we compare in this study depend on wind speed (u) and the Schmidt number (Sc), which depends on temperature (T). The Schmidt number (Sc) is a dimensionless number defined as the ratio of momentum diffusivity (v) and mass diffusivity (D), i.e., $Sc = v/D$ (Liss and Merlivat, 1986). The DMS sea-air flux is determined by using a bulk flux equation $F = k(C_w - C_a/H)$ where F is the calculated DMS flux, k is the gas transfer velocity, and C_w and C_a are the concentrations of the DMS in the seawater and the atmosphere adjacent to the seawater respectively (Wanninkhof, 2014). H is Henry's law solubility for DMS in seawater, which varies with temperature, which is given as $ln\ H = -3547/T + 12.64$ (Dacey

https://doi.org/10.5194/egusphere-2024-175
Preprint. Discussion started: 27 February 2024

and Wakeham, 1984). Here, C_a and C_w are measured in situ, while *k* depends on wind speed. C_w is several orders of magnitude higher than C_a; hence C_a/H is often ignored (Yan et al., 2023). The seven parameterizations discussed give estimates of the *k* and *Sc* values.

As wind is one of the most influential factors affecting gas transfer, most parameterizations have established different wind speed regimes for which different equations estimate the *k* values. The gas transfer velocity *k* results from the waterside transfer velocity (k_w) and airside transfer velocity (k_a). For the rarely soluble gas, airside resistance is usually small and neglected, but DMS solubility increases with a decrease in temperature, and hence, air resistance becomes important (Lana et al., 2011; Marandino et al., 2009; Omori et al., 2017). Most parameterizations agree that at wind speeds less than 3.6 m s^{-1}, the surface is generally smooth with few waves, known as the 'smooth surface regime.' When the wind speed is above 3.6 m s^{-1} but less than 13 m s^{-1}, it is 'rough surface regime,' and more waves are observed, enhancing the gas transfer. Above 13 m s^{-1} is known as the 'breaking wave regime,' where bubbles are formed along with the waves, significantly increasing the flux as evident from the Heidelberg circular wind tunnel experiments (Jähne et al., 1984; Jahne et al., 1979; Liss and Merlivat, 1986). The different flux parameterizations estimate the k value in those different wind regimes ($u \leq 3.6$: smooth surface regime, $3.6 < u \leq 13$: rough surface regime, $u > 13$: breaking wave regime), and these wind regimes are also dependent on the Schmidt number (*Sc*) for each parametrization, where Schmidt number depends on temperature (T).

2.1 Flux parameterization methods

2.1.1 LM86 Flux Parametrization

LM86 formulated the following equations for the three wind regimes, which are defined below following the results of the Heidelberg experiments (Jahne et al., 1979; Jähne et al., 1984) :

$$k_{lm86} = 0.17 \times \left(600/_{Sc}\right)^{2/3} \times u \qquad (u \leq 3.6) \qquad (1)$$

$$k_{lm86} = \left(600/_{Sc}\right)^{1/3} \times (2.85 \times u - 10.26) + 0.61 \times \left(600/_{Sc}\right)^{2/3} \qquad (3.6 < u \leq 13) \qquad (2)$$

$$k_{lm86} = \left(600/_{Sc}\right)^{1/3} \times (5.9 \times u - 49.91) + 0.61 \times \left(600/_{Sc}\right)^{2/3} \qquad (u > 13) \qquad (3)$$

Here, *u* is the wind speed in m s^{-1} at 10 m above the sea surface. The *Sc* is based on the work carried out by Saltzman *et al.* (1993) and the references therein for the temperature range from 5° C to 30° C using:

$$Sc = 2674 - (147.12 \times SST) + (3.726 \times SST^2) - (0.038 \times SST^3) \qquad (4)$$

2.1.2 E93 Flux Parameterization

Erickson (1993) assumed that the sea surface is a mixture of a low-turbulence area (non-whitecap) and a high-turbulence area (whitecap). The gas transfer velocities are obtained from the radon outgassing data obtained during the expedition of Transient Tracers in the Ocean (TTO) and Geochemical Ocean Sections Study (GEOSECS) (Monahan and Spillane, 1984; Kettle and

https://doi.org/10.5194/egusphere-2024-175
Preprint. Discussion started: 27 February 2024

Andreae, 2000). The gas transfer velocities for other species are calculated using the following conversion formula based on wind speed ranges:

$$k_{e93} = k_{R_n} \times \left({Sc}/{Sc_{R_n}}\right)^{-2/3} \quad (u < 3.6) \quad (5)$$

$$k_{e93} = k_{R_n} \times \left({Sc}/{Sc_{R_n}}\right)^{-1/3} \quad (u \geq 3.6) \quad (6)$$

Here, k_{Rn} (Monahan and Spillane, 1984) and Sc_{Rn} are the gas transfer velocity and Schmidt number for radon, respectively, which are given as follows:

$$k_{R_n} = 2.3 + 1.25 \times 10^{-3} \times u^3 \quad (u \text{ in m d}^{-1}) \quad (7)$$

$$Sc_{R_n} = 3147.3 - 201.9 \times SST + 5.5 \times SST^2 - 0.055 \times SST^3 \quad (8)$$

2.1.3 N00a and N00b Flux Parametrization

Dual tracer methods (Watson et al., 1991) involving the measurements of sulfur hexafluoride SF_6 and 3-Helium (^3He) were also used to estimate *k* (Watson et al., 1991). Nightingale et al. (2000) describe the ideal dual tracer combination as the one with one of the tracers being non-volatile, allowing dilution and dispersion corrections to be applied to the volatile tracer to minimize errors while estimating *k*. Due to the absence of such an ideal marine tracer, Nightingale et al. (2000) introduced a novel method of adding metabolically inactive bacterial spores of *Bacillus globigii* var. *Niger* as a conservative tracer to study the gas exchange in the North Sea (Watson et al., 1991; Nightingale et al., 2000) along with SF_6 and ^3He dual tracer for comparison. Combining data from other studies in George's Bank (Wanninkhof et al., 1993) and the West Florida shelf (Wanninkhof et al., 1997) with the North Sea data, the N00a parameterization coefficient was given as

$$k_{n00a} = (0.222 \times u^2 + 0.333 \times u) \times \left({Sc}/{600}\right)^{-0.5} \quad (9)$$

However, this study exclusively had data from the Northern Atlantic region. Coale et al. (1996) reported *k* values by using the dual tracer ($SF_6/^3He$) in the equatorial Pacific Ocean, which was then used to upgrade the N00a parameterization to N00b; the upgraded parameterization is given as

$$k_{N00b} = (0.222 \times u^2 \times shape\ parameter + 0.333 \times \mathrm{u}) \times \left({Sc}/{600}\right)^{-0.5} \quad (10)$$

Here, the *shape parameter* is used to describe variations in wind speed using Weibull Distribution.

2.1.4 Ho06 Flux Parameterization

https://doi.org/10.5194/egusphere-2024-175
Preprint. Discussion started: 27 February 2024

Ho et al. (2006) applied the dual tracer technique to measure the gas transfer velocity with the wind speed ranging from 7–16 m s^{-1}. This was done during the Surface Ocean Lower Atmosphere Study (SOLAS) Air-Sea Gas Exchange (SAGE) campaign. The estimation of Ho06 was derived from the SAGE data, and the gas transfer coefficient is given as,

$$k_{ho06} = (0.266 \pm 0.019) \times u^2 \quad (11)$$

2.1.5 GM12 Flux Parametrization

Goddijn-Murphy et al. (Goddijn-Murphy et al., 2012) argued that since the wind does not directly affect the gas transfer, it is the turbulence caused due to wind that helps to form bubbles, which increases gas transfer. Hence, the sea-surface roughness is a better parameter to quantify gas transfer. This study used satellite altimetry data to understand the sea surface roughness and measured DMS gas transfer velocity using the eddy covariance flux determination from eight cruises. This resulted in the new GM12 parameterization, which gives gas transfer velocity given as,

$$k_{gm12} = 2.1 \times u - 2.8 \quad (12)$$

2.1.6 W14 Flux Parametrization

Wanninkhof (1992) used the radiocarbon ^{14}C data from the Red Sea (Cember, 1989) to understand the CO_2 gas exchange rates. Based on this, the parametrization was developed using *Sc* number related to the work carried out by Saltzman *et al.* (1993) with the temperature range between 18° C to 25° C. Further, with the help of better quantification of global wind fields and using data with a broader temperature range (-2° C to 40° C), the parametrization developed in 1992 is being upgraded using revised global ocean ^{14}C inventories and improved wind speed product. This new parametrization technique is known as W14, which gives a gas transfer velocity equation:

$$k_{w14} = 0.251 \times u^2 \times \left(Sc_{w14}/660\right)^{-0.5} \quad (13)$$

Here:

$$Sc_{w14} = 2855.7 - 177.63 \times SST + 6.0438 \times SST^2 - 0.11645 \times SST^3 + 0.00094743 \times SST^4 \quad (14)$$

2.2 Estimation of uncertainties

The total uncertainty in DMS fluxes (σ_{total}) is calculated using the standard deviations in seawater DMS concentration (σ_{DMS}), coefficient of parameterization (σ_k), and wind speed (σ_{wind}):

$$\sigma_{total} = \sqrt{\sigma_{DMS}^2 + \sigma_k^2 + \sigma_{wind}^2} \quad (15)$$

The flux due to σ_{DMS} is computed for each pixel using the standard deviation between the seawater DMS concentrations of H22, W20, and G18, which is then passed through the N00b parametrization. The flux due to σ_k is calculated by calculating the standard deviation between the coefficients of all seven flux parameterizations. The flux due to σ_{wind} is computed using

https://doi.org/10.5194/egusphere-2024-175
Preprint. Discussion started: 27 February 2024

standard deviation between monthly global wind data from the different sources (NCEP Reanalysis 1, NCEP/DOE Reanalysis 2, ECMWF Reanalysis v5 (ERA5)), and then it is passed through N00b parameterization. Here, N00b is chosen as it has been used historically in previous studies (Simó and Dachs, 2002; Lana et al., 2011; Hulswar et al., 2022; McNabb and Tortell, 2022; Zhang et al., 2021; Zhao et al., 2003) for the calculation of fluxes. Finally, σ_{total} is obtained using Eq.(15).

3 Results and discussion

3.1 Salient features and seasonal variations

We estimated the seasonal DMS flux using seven different parameterizations and the global seawater DMS data of H22 (Fig.1), G18 (Fig.S1), and W20 (Fig.S2) climatologies to study the geographical and seasonal variations and the differences between the parameterizations.

Overall, the fluxes estimated using all seven parameterizations follow the seawater DMS concentration distribution, with higher values in the southern/northern hemispheres during their respective summers (Fig.1). Elevated levels are also seen in the Indian, Atlantic, and Pacific Oceans in the extra-tropical regions, where elevated wind speed causes higher sea-air fluxes. While the geographical patterns are similar, there is a large difference in the absolute values between the different parameterizations. When using the G18 or W20 seawater DMS concentrations, the emissions show a similar difference between the different parameterizations, although the absolute values are lower (Fig.S1 and S2).

In December-January-February (DJF), E93 shows a maximum DMS flux of 45.82 µmol m^{-2} d^{-1} in the Weddell Sea region, where the maximum DMS concentration of 18.67 nM is also observed in H22 (Joge: Part A). For E93, the flux is more uniformly distributed across the Southern Ocean as compared to the other parameterizations (Fig.1). The other parameterizations also show elevated values in the Southern Ocean, although the range depends on the parameterization used. For example, the E93 parameterization results in the highest values, exceeding 20 µmol m^{-2} d^{-1} throughout the Southern Ocean, while the LM86 parameterization results in peak values less than 10 µmol m^{-2} d^{-1}. Further north, in other ocean basins such as the Indian Ocean Ho06, and N00b predict relatively higher fluxes than E93.

During March-April-May (MAM), most parameterizations predict elevated fluxes in the North Atlantic Ocean, Caribbean Sea, Baltic Sea, and North Sea, with the DMS flux ranging from 8.71 to 18.73 µmol m^{-2} d^{-1} using the H22 seawater DMS concentrations. Higher fluxes are also observed on the western coast of the American continent and in the coastal regions of Africa. The gyres in the equatorial Pacific and Indian Oceans also show higher fluxes, although the Northern Atlantic Ocean has higher fluxes than the other ocean basins. Although all the parameterizations show higher values in the northern hemisphere, E93 shows the relatively highest fluxes, and the LM86 parameterization shows the lowest fluxes. In a similar manner, N00b shows high flux values (13.8 µmol m^{-2} d^{-1}) compared to N00a (11.33 µmol m^{-2} d^{-1}) in the Caribbean Sea, probably due to the wind correction factor in N00b parametrization.

June-July-August (JJA) period shows high values in the upwelling regions off the continental coasts and the equatorial Indian Ocean and Pacific Ocean. During this period, the geographical variation strongly depends on the parameterization chosen. For

https://doi.org/10.5194/egusphere-2024-175
Preprint. Discussion started: 27 February 2024

example, the E93 parameterization mainly shows peaks in the Arctic Ocean and the northern boundaries of the other ocean basins. However, others show peaks in the equatorial oceans in addition to the northern latitudes. This difference in variation is driven by the different sensitivity of the parameterizations to winds.

Flux values start increasing in the Southern Ocean during September-October-November (SON). The flux value estimated by Ho06 were the highest during this period (18.40 µmol m^{-2} d^{-1}) in the south Atlantic Ocean near the coast of South Africa, although the other parameterizations also show an increase in the Southern Ocean except for LM86. A distinct hotspot is also seen in the Indian Ocean region in all estimations such as Ho06 followed by N00a (13.77 µmol m^{-2} d^{-1}), N00b (16.75 µmol m^{-2} d^{-1}), GM12 (11.97 µmol m^{-2} d^{-1}), and W14 (13.84 µmol m^{-2} d^{-1}), while LM86 estimated the least (10.66 µmol m^{-2} d^{-1}) in the Indian ocean region.

3.2 Differences

We calculated the seasonal differences between all the flux parameterizations with respect to the N00b (Fig.2), which is still one of the most commonly used parameterizations (Lana et al., 2011; Hulswar et al., 2022). Annually, the largest positive difference is seen in the LM86 parameterization, which consistently displays lower values than the N00b parametrization. The largest negative differences in the polar regions are observed in the E93 parameterization, which shows that higher values are calculated at those regions than the N00b parameterization. Although Ho06 also shows large negative differences in the polar regions, large positive differences are observed in the mid-latitude and coastal regions. These differences can be as much as 100 % in certain regions, showing that the choice of parameterization plays a crucial role in the DMS flux estimates.

The largest positive differences (8.10 µmol m^{-2} d^{-1} in DJF, 5.15 µmol m^{-2} d^{-1} in MAM, 14.29 µmol m^{-2} d^{-1} in JJA and 6.11 µmol m^{-2} d^{-1} in SON) are observed in N00b-LM86, while the largest negative differences (-38.93 µmol m^{-2} d^{-1} in DJF, -14.48 µmol m^{-2} d^{-1} in MAM, -11.32 µmol m^{-2} d^{-1} in JJA and -10.61 µmol m^{-2} d^{-1} in SON) are with E93. This large negative difference is driven by the differences in the high latitude regions where N00b does not show significant peaks, for example, in the Southern Ocean (Fig.1). In the mid-latitude and the equatorial regions, significant peaks are observed in N00b estimations and hence N00b-E93 shows largest positive difference of 8.18 µmol m^{-2} d^{-1} in DJF, 6.32 µmol m^{-2} d^{-1} in MAM both in the Caribbean Sea, 18.45 µmol m^{-2} d^{-1} in JJA in the Indian Ocean near the coast of Somalia, and 6.81 µmol m^{-2} d^{-1} in SON in the Indian Ocean near Mauritius.

Although N00b is upgraded from N00a parameterization, there is no negative difference between the two parametrizations (Fig.2), which indicates that N00b estimates higher flux values than N00a everywhere (Fig.1). The maximum positive differences between the two range from 2.47 µmol m^{-2} d^{-1} in MAM in the Caribbean Sea to 6.12 µmol m^{-2} d^{-1} in JJA in the Indian Ocean near Somalia. The differences between N00b and Ho06 are primarily negative and range from -3.92 µmol m^{-2} d^{-1} to -10.59 µmol m^{-2} d^{-1} in the Southern Ocean, while positive differences are lower than N00b-N00a and the range is from 1.5 to 2.37 µmol m^{-2} d^{-1}.

The difference between N00b and GM12 is positive. Seasonally, the maximum positive difference is 16.17 µmol m^{-2} d^{-1} in JJA in the Indian Ocean near Somalia, 4.37 µmol m^{-2} d^{-1} in MAM, and 5.93 µmol m^{-2} d^{-1} in DJF in the Caribbean Sea, 4.94

https://doi.org/10.5194/egusphere-2024-175
Preprint. Discussion started: 27 February 2024

μmol m^{-2} d^{-1} in SON in the Indian Ocean near Mauritius. Similarly, in the case of N00b-W14, significant positive differences are observed. The maximum difference of 4.52 μmol m^{-2} d^{-1} in JJA in the Indian Ocean near Somalia, 2.59 μmol m^{-2} d^{-1} in MAM in the North Sea, 4.12 μmol m^{-2} d^{-1} in DJF in the Ross Sea and 2.93 μmol m^{-2} d^{-1} in SON in the Indian Ocean near Mauritius can be seen from Figure 2. Flux estimated with W14 parameterization shows positive differences with N00b with minimum difference of 0.04 μmol m^{-2} d^{-1} and maximum difference of 4.52 μmol m^{-2} d^{-1}.

3.3 Drivers in flux uncertainties

As explained in the methods section, the total uncertainty in DMS fluxes is driven by the uncertainty in the seawater DMS concentrations, parameterization, and wind speed.

Figure S3 shows the standard deviation in the DMS flux calculated using the standard deviation between climatological seawater DMS concentrations (σ_{DMS}) of G18, W20, and H22. Here, the sea-air parameterization is kept constant to isolate the effect of the change due to seawater DMS concentrations (we use N00b for this calculation). The monthly climatological wind speed data (NCEP reanalysis 1) is used for the flux estimation. In DJF, the maximum standard deviation of 34.64 μmol m^{-2} d^{-1} is observed in January near the coast of Namibia in the South Atlantic Ocean, while high values of up to 28.76 μmol m^{-2} d^{-1} are observed near the coast of South Africa of South Atlantic Ocean. In JJA, a maximum standard deviation of 23.87 μmol m^{-2} d^{-1} is observed near the coast of Oman in the Arabian Sea in July, while high values up to 21.86 μmol m^{-2} d^{-1} are seen around the same region in August. During the MAM season, the maximum σ_{DMS} (20.55 μmol m^{-2} d^{-1}) is observed May near the Gulf of Kutch of Arabian Sea, while in SON, the maximum σ_{DMS} (18.40 μmol m^{-2} d^{-1}) is observed in the South Atlantic Ocean near the coast of Namibia. Overall, the largest standard deviation in σ_{DMS} is in the Southern Ocean, where the DMS concentrations are the largest.

Figure S4 shows the standard deviation in the DMS flux due to the different flux parameterizations (σ_k). Here, we keep the seawater DMS concentrations constant (H22), and monthly climatological wind speed data of NCEP reanalysis 1 is used. In DJF season, large σ_k values ranging between 6.99 to 21.70 μmol m^{-2} d^{-1} are observed in the regions close to the Antarctic Peninsula. In JJA, large values between 5.75 to 8.86 μmol m^{-2} d^{-1} are observed in the Somali basin of the Indian Ocean. In MAM, this peak range is from 3.17 to 9.12 μmol m^{-2} d^{-1} in the South Atlantic Ocean near Congo Canyon, the Baltic Sea, and the Prince of Wales near the Gulf of Alaska. In SON, the peak σ_k ranges between 2.93 to 10.43 μmol m^{-2} d^{-1} in the Somalian basin, Bay of Bengal, and the Antarctic region. Annually averaged, the maximum σ_k value of 5.35 μmol m^{-2} d^{-1} is obtained around Antarctica in the Southern Ocean.

Further, the standard deviation in the DMS flux is estimated again with the standard deviation in wind speed (σ_{wind}), which is obtained through the standard deviation between monthly wind speed data from different sources (NCEP reanalysis 1, NCEP/DOE reanalysis 2, ERA5), with the seawater DMS concentration of H22 and a flux parameterization equation (N00b). The area weighted global mean flux standard deviation due to σ_{wind} was much lower than the area weighted global mean flux std due to σ_{DMS} and σ_k on monthly and annual scales (Table 1). The maximum annual average of 2.62 μmol m^{-2} d^{-1} due to

https://doi.org/10.5194/egusphere-2024-175
Preprint. Discussion started: 27 February 2024

σ_{wind} is obtained near the Cape Adare of Antarctica. This shows that the total standard deviation of the sea-air DMS flux (σ_{total} is calculated using Eq.(15)) is dominated by σ_{DMS} and σ_k, with σ_{wind} playing a minor role in the total flux uncertainty (Table 1). The climatological monthly and annual σ_{total} are shown in Figure 3. In DJF, the maximum σ_{total} observed is 22.66 µmol m^{-2} d^{-1} in the regions close to the Antarctic Peninsula. In JJA, the maximum σ_{total} was 24.60 µmol m^{-2} d^{-1} near coastal Oman in the Arabian Sea. In MAM, the higher values of σ_{total} range between 12.68 to 17.17 µmol m^{-2} d^{-1}, with the highest value in the North Atlantic Ocean near Western Sahara. In SON, the highest σ_{total} is 16.47 µmol m^{-2} d^{-1}, in the South Atlantic Ocean near the west coast of South Africa. At an annual scale, the maximum total deviation is 8.55 µmol m^{-2} d^{-1}, is observed in the North Atlantic ocean near the coast of Mauritania, although the Southern Ocean also shows significant values of σ_{total} along with coastal regions of South America and Africa.

As mentioned above, the σ_{total} of DMS flux is dominated by σ_{DMS} and σ_k, with σ_{wind} having a minor contribution (Table 1). In Figure 3, the regions where the σ_{total} is dominated by the variation in seawater DMS concentrations, i.e., $\sigma_{DMS} > \sigma_k$, are indicated by red dots. The regions where the red dots are absent are the ones where the dominant contribution to σ_{total} is due to σ_k. It is observed that σ_{total} in oligotrophic oceans and most of coastal areas are dominated by σ_{DMS}. Annually, the σ_{total} in the Southern Ocean is dominated by $\sigma_{DMS,}$ but the coastal area of Antarctica is dominated by σ_k. Table 1 also shows the total DMS_{sulfur} flux to the atmosphere according to each month and annually averaged. For most of the year, the total flux from regions where σ_{DMS} is greater than σ_k is larger. Indeed, the total annual flux of DMS_{sulfur} to the atmosphere is estimated as 22.08 Tg, of which 17.16 Tg is contributed by areas where $\sigma_k < \sigma_{DMS}$. This indicates that on an annual scale, the uncertainty in DMS_{sulfur} emissions is dominated by seawater DMS concentration. However, from Figure 3, the choice of the flux parametrization also contributes a significant amount of uncertainty in coastal areas of Antarctica, which can be observed in November, December, January, and February. Overall, the choice of seawater DMS estimation method has larger influence on sea-air DMS flux than the choice of flux parameterization (Bhatti et al., 2023).

3.4 Comparison with in situ observations

In situ DMS flux data measured by eddy covariance or gradient flux techniques was obtained from various studies carried out over the global oceans (Table S1). These were compared with the co-located DMS flux data estimated from different parameterizations using the W22 (Fig.4), G18 (Fig.S5), and W20 (Fig.S6). In this analysis, the in situ DMS flux data is monthly binned to 1º × 1º spatial resolution as the estimated DMS flux climatologies are also at the same resolution, and then ordinary least square regression is applied. For reference, raw in situ DMS flux points are shown in the background (Fig.4, S5 and S6). All flux estimates using either of the DMS seawater climatologies, with any of the flux parameterizations, struggle to match the observations.

In most cases, the flux estimations in the lower range (< 20 µmol m^{-2} d^{-1}) are overestimated, while the values are underestimated in the higher range (> 20 µmol m^{-2} d^{-1}). Indeed, in all the cases, a positive intercept in the linear regressions shows that the emissions are overestimated at lower flux values. This would indicate a constant background flux in the estimated emissions,

https://doi.org/10.5194/egusphere-2024-175
Preprint. Discussion started: 27 February 2024

which would overestimate the total DMS_{sulfur} flux to the atmosphere. In contrast, the fact that the flux estimates do not reproduce the higher DMS fluxes indicates that high emission scenarios, which would contribute strongly to new particle formation and growth, are underestimated by the emission estimations. It should be noted that we use monthly seawater DMS concentration fields as input. Hence, a difference between the observations and estimations is expected, but a consistent difference in lower and higher ranges points to emissions being overestimated/underestimated in models. The best match in the lower range is found when using the W20 seawater DMS estimations (Fig.S6), although the slope is consistently lower than 0.33, and the intercept is higher than 2.17 for all the flux parameterizations (R^2<0.32 for all the parameterizations). Both H22 and W20 perform ~~relatively~~ better than G18, but none of the correlation coefficients are found to be significant, and all the flux parametrization methods fail to reproduce the in situ DMS flux values, particularly the high values of fluxes. (Fig.4, S5 and S6).

4 Conclusions

The sea-air DMS flux was estimated using different seawater DMS climatologies (see Joge: Part A), wind, and SST as input to seven different flux parameterizations. All the flux estimations show a similar seasonal variation, with peaks in the summers of each hemisphere. However, there were large geographical and absolute flux differences between the different estimations, showing that the DMS_{sulfur} flux to the atmosphere is sensitive to the chosen seawater DMS fields and the chosen flux parameterization. The total uncertainty in flux estimation is dominated by the uncertainty in seawater DMS concentrations and the choice of flux parametrization, while the effect on the total uncertainty due to ~~standard deviation between~~ the different sources of wind data is not as significant; however, this might not be true when comparing to in situ fluxes as the gustiness of wind might play an important role. In certain parts of the globe, such as Peru upwelling region, the South Pacific Ocean, Indian Ocean, Arabian Sea, Bay of Bengal, Coastal areas of continents, North Atlantic Ocean, Gulf of Alaska, and Southern Ocean, etc., the differences between the climatological estimated DMS of G18, W20, H22 can be observed (Paper: Part A). Hence, the uncertainty in total flux emission is dominated by uncertainty due to seawater DMS concentration in these areas where the differences are significant (Fig.3). In other regions, it is dominated by choice in coefficient of flux parametrization, such as the coastal area of Antarctica and the Arctic Ocean. Comparison of in situ and co-located estimated flux show that all the estimations overestimate the DMS flux below 20 µmol m^{-2} d^{-1} but underestimate fluxes larger than 20 µmol m^{-2} d^{-1}. This suggests that emissions in current models overestimate the total sea-air DMS flux but underestimate the higher range when it can significantly impact new particle formation and growth.

Code availability

Codes for the analysis and figures are available on request.

Data availability

https://doi.org/10.5194/egusphere-2024-175
Preprint. Discussion started: 27 February 2024

All the data used here are publicly available and links are provided in the manuscript.

Competing Interests

The authors declare that they have no conflict of interest.

Author Contributions

ASM conceptualized the study. SJ analyzed the data with help from SH. CM, MG, MY, TB and RS helped with the data, ideas and understanding of the study. SJ and ASM wrote the manuscript with the help of all the coauthors.

Acknowledgements

The Indian Institute of Tropical Meteorology is funded by the Ministry of Earth Sciences, Government of India. MG and RS acknowledge support from the European Research Council (ERC) under the European Union's Horizon 2020 research and innovation program (grant agreement #834162, SUMMIT Advanced Grant to RS), and the Spanish Government through grant GOOSE (PID2022_140872NB_I00) as well as the "Severo Ochoa Centre of Excellence" accreditation grant CEX2019-000928-S.

References

Andreae, M. O. and Crutzen, P. J.: Atmospheric aerosols: Biogeochemical sources and role in atmospheric chemistry, Science (80-.)., 276, 1052–1058, 1997.

Andreae, M. O. and Raemdonck, H.: Dimethylsulfide in the surface ocean and the marine atmosphere: A Global View, Science (80-.)., 221, 744–747, 1983.

Bhatti, Y. A., Revell, L. E., Schuddeboom, A. J., Mcdonald, A. J., Archibald, A. T., Williams, J., Venugopal, A. U., Hardacre, C., Behrens, E., and Bhatti, Y.: The sensitivity of Southern Ocean atmospheric dimethyl sulfide to modelled sources and emissions, 15181–15196, 2023.

Carpenter, L. J., Archer, S. D., and Beale, R.: Ocean-atmosphere trace gas exchange, Chem. Soc. Rev., 41, 6473–6506, https://doi.org/10.1039/c2cs35121h, 2012.

Cember, R.: Bomb radiocarbon in the Red Sea: A medium-scale gas exchange experiment, J. Geophys. Res., 94, 2111, https://doi.org/10.1029/JC094iC02p02111, 1989.

Charlson, R. J., Lovecook, J. E., Andreae, M. O., and Warren, S. G.: Ocean phytoplankton, atmospheric sulfur, cloud albdeo and climate, Nature, 326, 655–661, https://doi.org/10.1029/2003GB002183, 1987.

Coale, K. H., Johnson, K. S., Fitzwater, S. E., Gordon, R. M., Tanner, S., Chavez, F. P., Ferioli, L., Sakamoto, C., Rogers, P., Millero, F., Steinberg, P., Nightingale, P., Cooper, D., Cochlan, W. P., Landry, M. R., Constantinou, J., Rollwagen, G., Trasvina, A., and Kudela, R.: A massive phytoplankton bloom induced by an ecosystem-scale iron fertilization experiment in

https://doi.org/10.5194/egusphere-2024-175
Preprint. Discussion started: 27 February 2024

the equatorial Pacific Ocean, Nature, 383, 495–501, https://doi.org/10.1038/383495a0, 1996.

Dacey, J. W. H. and Wakeham, G.: HENRY'S LAW CONSTANTS FOR DIHETHYLSULFIDE IN FRESHWATER AND SEAWATER, 11, 991–994, 1984.

Erickson, D. J.: A stability dependent theory for air-sea gas exchange, J. Geophys. Res. Ocean., 98, 8471–8488, https://doi.org/10.1029/93JC00039, 1993.

Galí, M., Levasseur, M., Devred, E., Simó, R., and Babin, M.: Sea-surface dimethylsulfide (DMS) concentration from satellite data at global and regional scales, 15, 3497–3519, https://doi.org/10.5194/bg-15-3497-2018, 2018.

Goddijn-Murphy, L., Woolf, D. K., and Marandino, C.: Space-based retrievals of air-sea gas transfer velocities using altimeters: Calibration for dimethyl sulfide, J. Geophys. Res. Ocean., 117, n/a-n/a, https://doi.org/10.1029/2011JC007535, 2012.

Ho, D. T., Law, C. S., Smith, M. J., Schlosser, P., Harvey, M., and Hill, P.: Measurements of air-sea gas exchange at high wind speeds in the Southern Ocean: Implications for global parameterizations, Geophys. Res. Lett., 33, L16611, https://doi.org/10.1029/2006GL026817, 2006.

Hulswar, S., Simó, R., Galí, M., Bell, T. G., Lana, A., Inamdar, S., Halloran, P. R., Manville, G., and Mahajan, A. S.: Third revision of the global surface seawater dimethyl sulfide climatology (DMS-Rev3), Earth Syst. Sci. Data, 14, 2963–2987, https://doi.org/10.5194/essd-14-2963-2022, 2022.

Ishii, M., Shouji, A., Sugimoto, S., and Matsumoto, T.: Objective analyses of sea-surface temperature and marine meteorological variables for the 20th century using ICOADS and the Kobe Collection, Int. J. Climatol., 25, 865–879, https://doi.org/10.1002/joc.1169, 2005.

Jahne, B., Münnich, K. O., and Siegenthaler, U.: Measurements of gas exchange and momentum transfer in a circular wind-water tunnel, 31, 321–329, https://doi.org/10.3402/tellusa.v31i4.10440, 1979.

Jähne, B., Münnich, K. O., and Siegenthaler, U.: Measurements of gas exchange and momentum transfer in a circular wind-water tunnel, Tellus A Dyn. Meteorol. Oceanogr., 31, 321, https://doi.org/10.3402/tellusa.v31i4.10440, 1979.

Jähne, B., Huber, W., Dutzi, A., Wais, T., and Ilmberger, J.: Wind/Wave-Tunnel Experiment on the Schmidt Number — and Wave Field Dependence of Air/Water Gas Exchange, in: Gas Transfer at Water Surfaces, Springer Netherlands, Dordrecht, 303–309, https://doi.org/10.1007/978-94-017-1660-4_28, 1984.

Kalnay, E., Kanamitsu, M., Kistler, R., Collins, W., Deaven, D., and Gandin, L.: The NCEP / NCAR 40-Year Reanalysis Project, Bull. Am. Meteorol. Soc., 437–472, https://doi.org/10.1175/1520-0477(1996)077<0437:TNYRP>2.0.CO;2, 1996.

Kettle, A. J. and Andreae, M. O.: Flux of dimethylsulfide from the oceans: A comparison of updated data sets and flux models, J. Geophys. Res. Atmos., 105, 26793–26808, https://doi.org/10.1029/2000JD900252, 2000.

Lana, A., Bell, T. G., Simó, R., Vallina, S. M., Ballabrera-Poy, J., Kettle, A. J., Dachs, J., Bopp, L., Saltzman, E. S., Stefels, J., Johnson, J. E., and Liss, P. S.: An updated climatology of surface dimethlysulfide concentrations and emission fluxes in the global ocean, Global Biogeochem. Cycles, 25, 1–17, https://doi.org/10.1029/2010GB003850, 2011.

Liss, P. S. and Merlivat, L.: Air-Sea Gas Exchange Rates: Introduction and Synthesis, in: The Role of Air-Sea Exchange in

Geochemical Cycling, vol. 1983, Springer Netherlands, Dordrecht, 113–127, https://doi.org/10.1007/978-94-009-4738-2_5, 1986.

Marandino, C. A., De Bruyn, W. J., Miller, S. D., and Saltzman, E. S.: Open ocean DMS air/sea fluxes over the eastern South Pacific Ocean, Atmos. Chem. Phys., 9, 345–356, https://doi.org/10.5194/acp-9-345-2009, 2009.

McNabb, B. J. and Tortell, P. D.: Improved prediction of dimethyl sulfide (DMS) distributions in the northeast subarctic Pacific using machine-learning algorithms, 19, 1705–1721, https://doi.org/10.5194/bg-19-1705-2022, 2022.

Monahan, E. C. and Spillane, M. C.: The Role of Oceanic Whitecaps in Air-Sea Gas Exchange, in: Gas Transfer at Water Surfaces, Springer Netherlands, Dordrecht, 495–503, https://doi.org/10.1007/978-94-017-1660-4_45, 1984.

Nightingale, D., Malin, G., Law, C. S., Watson, J., Liss, S., and Liddicoat, I.: In situ evaluation of air-sea gas exchange parameterizations using novel conservative and volatile tracers., Global Biogeochem. Cycles, 14, 373–387, https://doi.org/10.1029/1999GB900091, 2000.

Omori, Y., Tanimoto, H., Inomata, S., Ikeda, K., Iwata, T., Kameyama, S., Uematsu, M., Gamo, T., Ogawa, H., and Furuya, K.: Sea-to-air flux of dimethyl sulfide in the South and North Pacific Ocean as measured by proton transfer reaction-mass spectrometry coupled with the gradient flux technique, J. Geophys. Res., 122, 7216–7231, https://doi.org/10.1002/2017JD026527, 2017.

Saltzman, E. S., King, D. B., Holmen, K., and Leck, C.: Experimental determination of the diffusion coefficient of dimethylsulfide in water, J. Geophys. Res., 98, 16481, https://doi.org/10.1029/93JC01858, 1993.

Simó, R.: Production of atmospheric sulfur by oceanic plankton : biogeochemical , ecological and evolutionary links, Trends Ecol. Evol., 16, 287–294, 2001.

Simó, R. and Dachs, J.: Global ocean emission of dimethylsulfide predicted from biogeophysical data, Global Biogeochem. Cycles, 16, 26-1-26–10, https://doi.org/10.1029/2001gb001829, 2002.

Wang, W. L., Song, G., Primeau, F., Saltzman, E. S., Bell, T. G., and Moore, K. K.: Global ocean dimethyl sulfide climatology estimated from observations and an artificial neural network, 17, 5335–5354, https://doi.org/10.5194/bg-17-5335-2020, 2020.

Wanninkhof, R.: Relationship between wind speed and gas exchange over the ocean, J. Geophys. Res., 97, 7373–7382, https://doi.org/10.1029/92JC00188, 1992.

Wanninkhof, R.: Relationship between wind speed and gas exchange over the ocean revisited, Limnol. Oceanogr. Methods, 12, 351–362, https://doi.org/10.4319/lom.2014.12.351, 2014.

Wanninkhof, R., Asher, W., Weppernig, R., Chen, H., Schlosser, P., Langdon, C., and Sambrotto, R.: Gas transfer experiment on Georges Bank using two volatile deliberate tracers, J. Geophys. Res., 98, 20237, https://doi.org/10.1029/93JC01844, 1993.

Wanninkhof, R., Hitchcock, G., Wiseman, W. J., Vargo, G., Ortner, P. B., Asher, W., Ho, D. T., Schlosser, P., Dickson, M.-L., Masserini, R., Fanning, K., and Zhang, J.-Z.: Gas exchange, dispersion, and biological productivity on the West Florida Shelf: Results from a Lagrangian Tracer Study, Geophys. Res. Lett., 24, 1767–1770, https://doi.org/10.1029/97GL01757, 1997.

Watson, A. J., Upstill-Goddard, R. C., and Liss, P. S.: Air–sea gas exchange in rough and stormy seas measured by a dual-

https://doi.org/10.5194/egusphere-2024-175
Preprint. Discussion started: 27 February 2024

tracer technique, Nature, 349, 145–147, https://doi.org/10.1038/349145a0, 1991.

Yan, S. B., Li, X. J., Xu, F., Zhang, H. H., Wang, J., Zhang, Y., Yang, G. P., Zhuang, G. C., and Chen, Z.: High-resolution distribution and emission of dimethyl sulfide and its relationship with pCO2 in the Northwest Pacific Ocean, Front. Mar. Sci., 10, 1–12, https://doi.org/10.3389/fmars.2023.1074474, 2023.

Zhang, M., Marandino, C. A., Yan, J., Wu, Y., Park, K., Sun, H., Gao, Z., and Xu, S.: Unravelling Surface Seawater DMS Concentration and Sea-To-Air Flux Changes After Sea Ice Retreat in the Western Arctic Ocean, Global Biogeochem. Cycles, 35, 1–15, https://doi.org/10.1029/2020GB006796, 2021.

Zhao, D., Toba, Y., Suzuki, Y., and Komori, S.: Effect of wind waves on air'sea gas exchange: proposal of an overall CO 2 transfer velocity formula as a function of breaking-wave parameter , Tellus B Chem. Phys. Meteorol., 55, 478–487, https://doi.org/10.3402/tellusb.v55i2.16747, 2003.

Tables :

Table 1. Area Weighted Global mean flux standard deviation for each month and annually due to σ_{DMS}, σ_k and σ_{wind}. Also, DMS_{Sulfur} emissions for each month and annually from the areas with $\sigma_{DMS} > \sigma_k$ and the area $\sigma_{DMS} < \sigma_k$ and the total emission across the globe is computed using the N00b flux parameterization and H22 DMS climatology.

Month	Area Weighted Global Mean Flux std. due to σ_{DMS} (µmol m^{-2} d^{-1})	Area Weighted Global Mean Flux std. due *to* σ_k (µmol m^{-2} d^{-1})	Area Weighted Global Mean Flux std. due to σ_{wind} (µmol m^{-2} d^{-1})	DMS_{Sulfur} emissions where $\sigma_{DMS} > \sigma_k$ (Tg)	DMS_{Sulfur} emissions where $\sigma_{DMS} < \sigma_k$ (Tg)	Total DMS_{Sulfur} emissions (Tg)
January	1.85	1.69	0.16	1.47	0.85	2.33
February	1.42	1.29	0.13	1.07	0.68	1.74
March	1.52	1.28	0.13	1.54	0.50	2.04
April	1.07	0.99	0.10	0.98	0.52	1.50
May	1.31	1.09	0.11	1.11	0.51	1.62
June	1.51	1.09	0.11	1.24	0.49	1.73
July	1.39	1.09	0.12	1.29	0.52	1.81
August	1.41	1.08	0.12	1.42	0.47	1.89
September	1.04	0.83	0.09	1.09	0.41	1.50
October	1.08	0.94	0.10	0.97	0.63	1.60
November	1.79	1.47	0.14	1.36	0.60	1.96
December	1.82	1.70	0.16	1.40	0.90	2.30
Annual	**1.44**	**1.21**	**0.12**	**17.16**	**4.93**	**22.08**

https://doi.org/10.5194/egusphere-2024-175
Preprint. Discussion started: 27 February 2024

Figures :

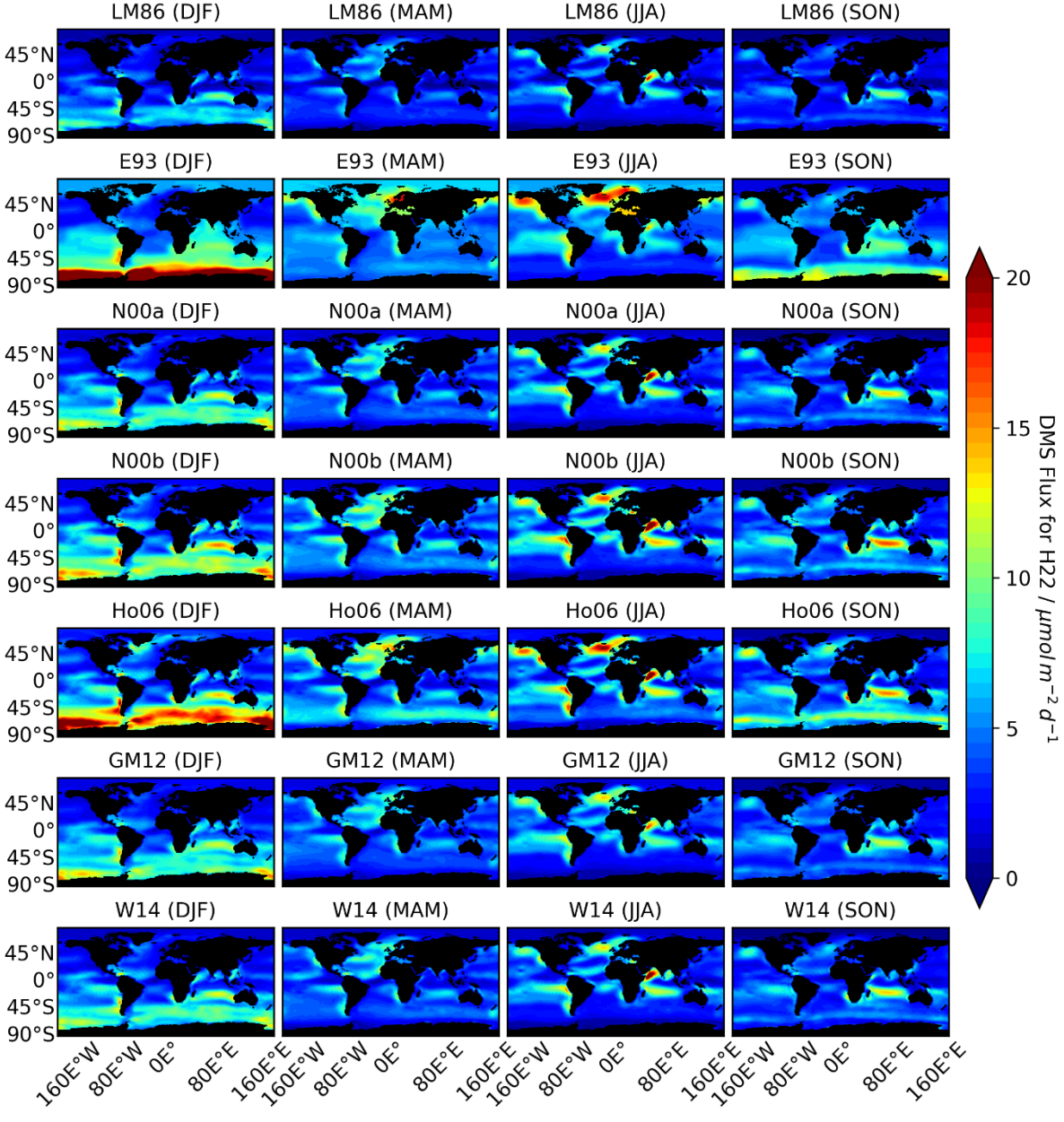

Figure 1: DMS fluxes estimated using the seven parameterizations for different seasons using the H22 climatology. The geographical pattern is similar in all the estimates, although the absolute values differ according to the parameterization chosen. In JJA, maximum flux of 33.75 μmol m^{-2} d^{-1} is observed in Indian ocean near Somalia with N00b. In DJF, maximum flux obtained 45.82 μmol m^{-2} d[illegible] Weddell Sea region with E93.

https://doi.org/10.5194/egusphere-2024-175
Preprint. Discussion started: 27 February 2024

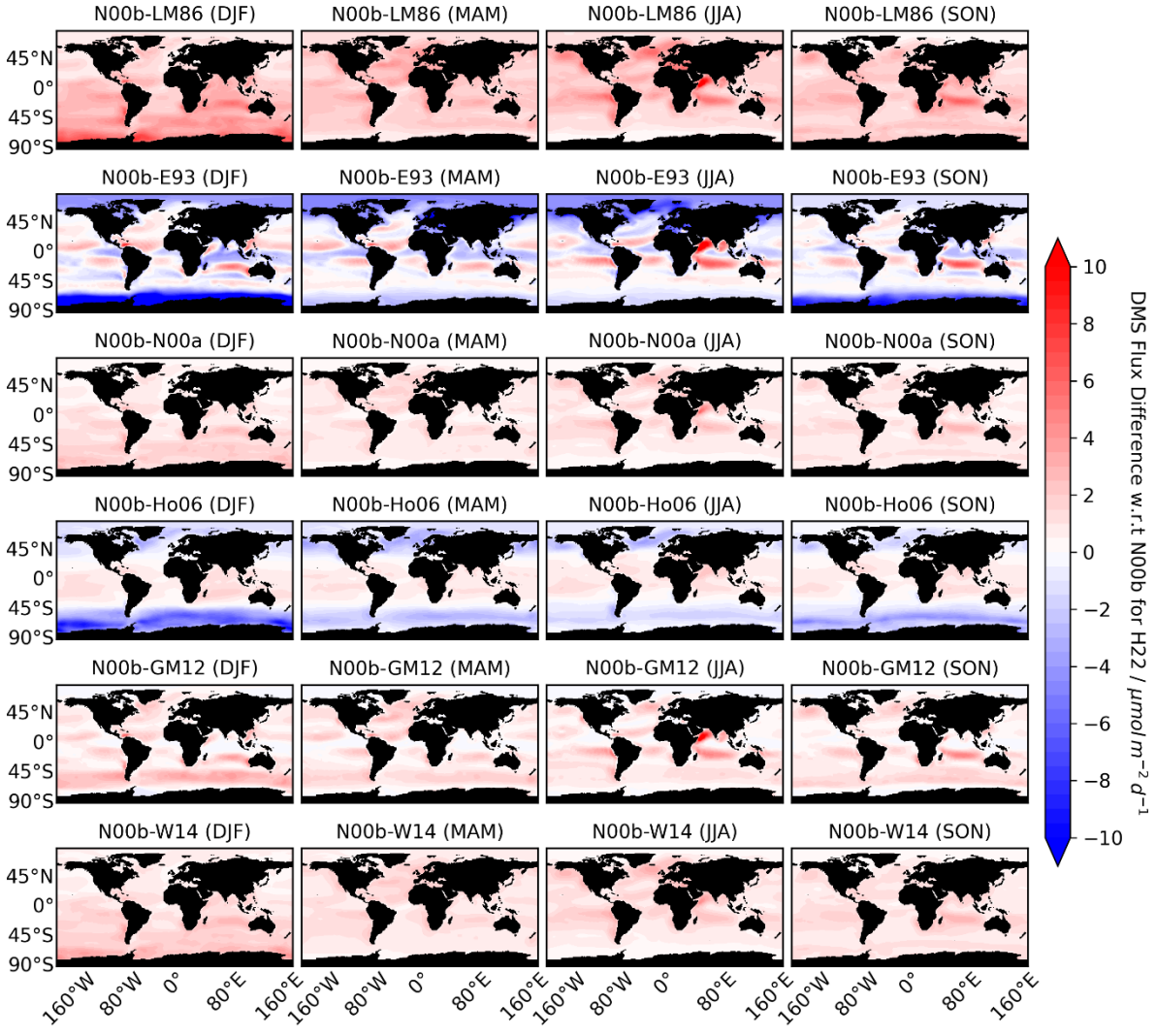

Figure 2: Differences between the DMS fluxes estimated using H22 with the N00b parameterization and the other seven parameters. For all the seasons, N00b-LM86 shows a positive difference, while the other parameterizations (E93, Ho06) show negative differences in the Southern Ocean and Arctic region, although some positive differences are also present in E93 and Ho06 in mid latitude regions. GM12, W14 and N00a show small positive differences with N00b while N00b-LM86 shows significant large positive difference.

https://doi.org/10.5194/egusphere-2024-175
Preprint. Discussion started: 27 February 2024

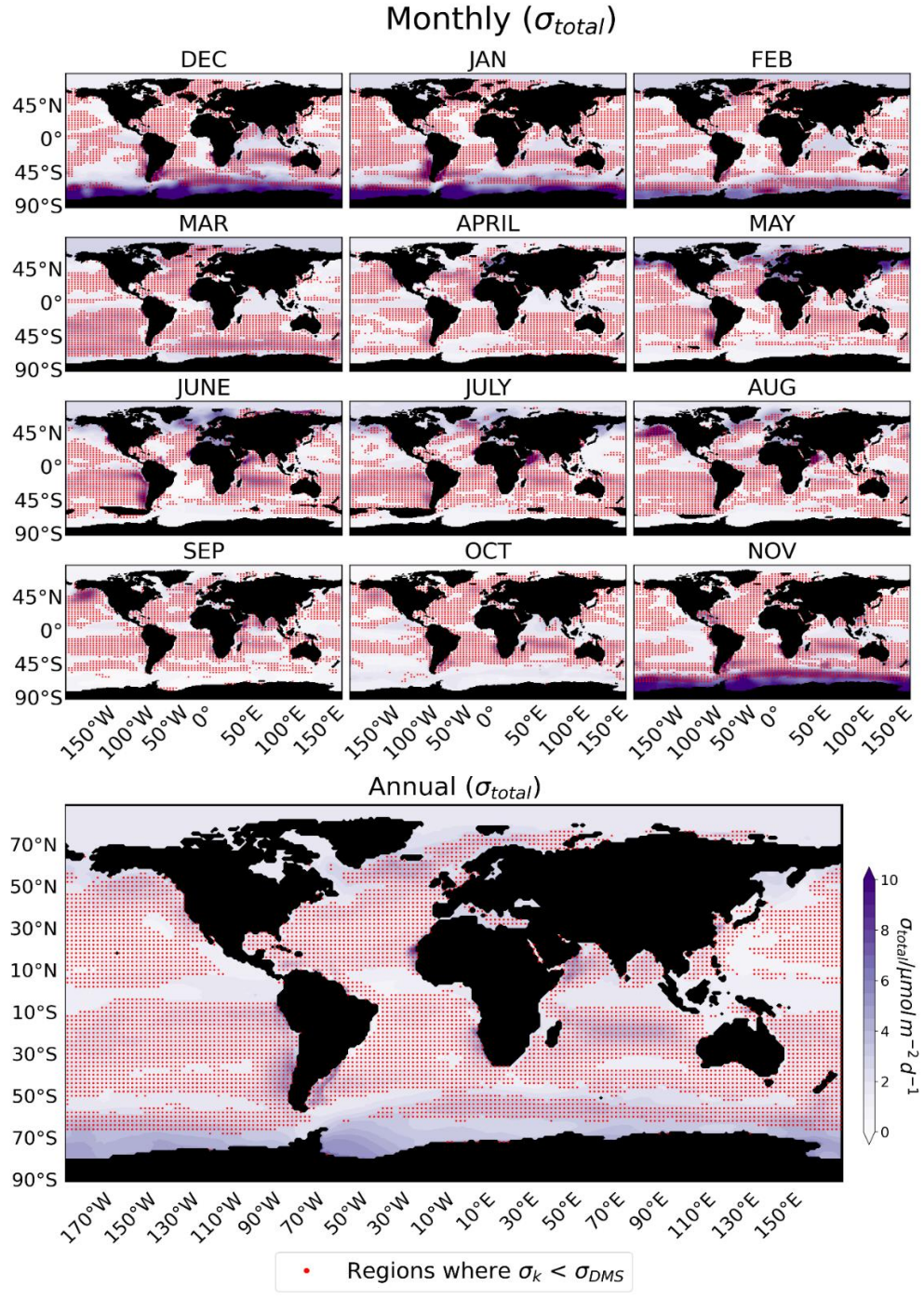

Figure 3: An estimate of the total variation (σ_{total}) in the flux emission, which is shown as a background map and is obtained from the standard deviations in the seawater DMS concentrations (σ_{DMS}), standard deviations in the coefficients of parametrizations (σ_k) and variation due to wind speed (σ_{wind}). σ_{wind} has a small contribution compared to σ_{DMS} and σ_k (Table 1). The regions where seawater DMS concentrations drive the uncertainty are indicated by red dots ($\sigma_{DMS} > \sigma_k$), while in the other areas (no red dots), it is driven by the variation due to the choice of the flux parameterization ($\sigma_{DMS} < \sigma_k$).

https://doi.org/10.5194/egusphere-2024-175
Preprint. Discussion started: 27 February 2024

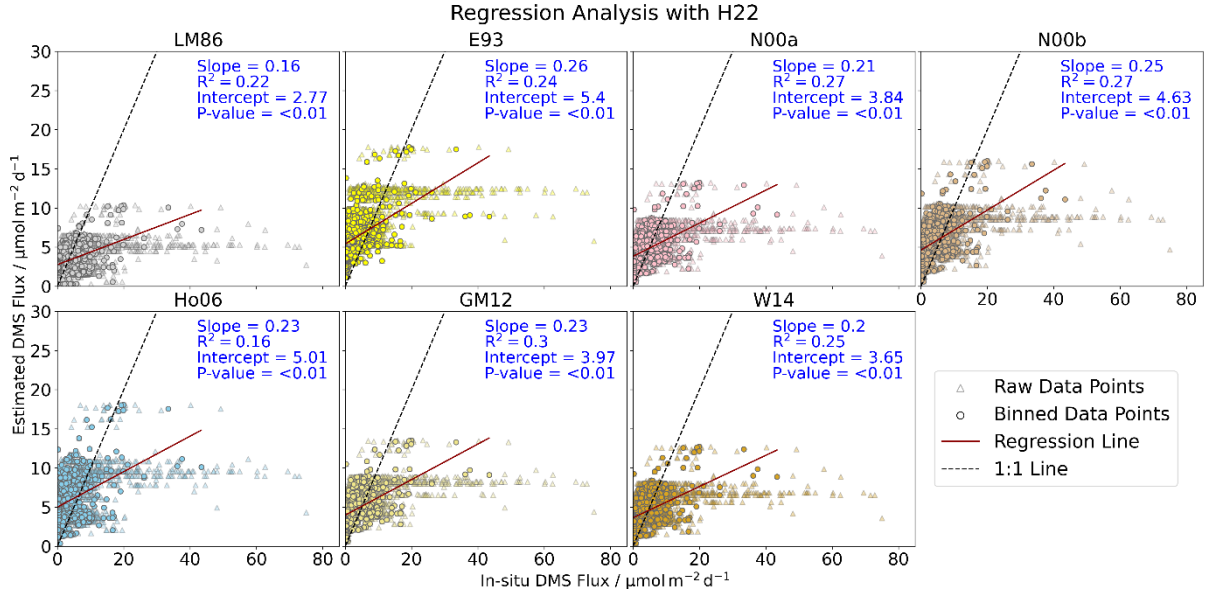

Figure 4: Comparison of in situ and estimated DMS fluxes (using H22) with the different parameterizations. Here, the regression analysis is done with binned in situ data at 1°×1° resolution, as the flux climatologies are also at the same resolution. Analysis shows that flux calculations result in higher fluxes than observations at low levels (< 20 µmol m^{-2} d^{-1}) and lower fluxes than observations at higher levels (> 20 µmol m^{-2} d^{-1}), which indicates that flux parametrization methods fail to represent high flux values. The black dash line is the 1:1 representation between in situ and the estimated DMS flux points, and the dark red line is the regression line. A list of the in situ observations used for the comparison is given in Table S1

Response to Reviewer 2 comments for manuscript ID egusphere-2024-175. The comments are given in an italic typeface, and the responses are given in a bold typeface. The corresponding changes in the revised manuscript are highlighted in red.

2.1) ***General comments:***

The manuscript provides a comparison of DMS emission field using three seawater DMS climatology and seven gas exchange parameterizations. The author then discusses the contribution of the differences in seawater DMS, gas exchange velocity, and wind speed to the DMS emission flux. Finally, the monthly emission estimates are validated using in-situ flux measurements. While DMS emission is an important topic and the results are useful, there are some issues that should be addressed to enhance its usefulness to the community.

Response: We thank the reviewer for thoroughly reviewing the manuscript. The answers to the detailed comments are given below.

2.2) ***Specific comments:***

2.1.1) L25: The ocean is the dominant source of global DMS emissions. However, DMS has also been found to be emitted from vegetation on land (e.g., (Vettikkat, et al. 2020)). The author should explore the literature and list the emission sources on land, which will give readers a broader perspective on DMS emissions across the Earth's surface.

Response: Yes, a line related to the DMS sources from vegetation on land is added and a reason why the ocean is a dominant source of DMS is given along with the relevant references (L36 – L39).

2.1.2) L58: Some other studies (e.g., (Blomquist, et al. 2017)) use equations which consider the bubble injection by breaking waves. Could you show some results using such equations and discuss the differences?

Response: Bubble bursting is an important process, but its impact on DMS emissions is not clear. It does affect sea salt aerosol formation, but describing these other processes, which are not directly relevant to DMS emissions, is beyond the scope of our topic.

2.1.3) L64: Please add a reference.

Response: Added (L85).

2.1.4) L76: Most of the transfer velocity parameterizations in this manuscript use transfer velocities measured for gases other than DMS. However, there are parameterizations derived directly from wind speed and DMS measurements (e.g., (Yang, et al. 2011)). It would be interesting to show the results using this kind of parameterization.

Response: Section 2.1.5 contains the Goddijn-Murphy et al. parametrization (GM12), which is a synthesis of k_{DMS} using (at that time) all available eddy covariance DMS flux observations. The data from Yang et. al. (2011) is included in this synthesis.

2.1.5) L130: (Wanninkhof 2014) should be cited here.

Response: Now included (L163).

2.1.6) L132: In (Wanninkhof 2014), the gas transfer velocity is given as: $k=0.251\times\langle U2\rangle\times(Sc/660)^{-0.5}$ *where,* $\langle U2\rangle$ *is the average of neutral stability winds at 10-m height squared, or the second moment. In the manuscript, the author uses monthly averaged*

wind speed. However, the difference between the two and the associated uncertainty in DMS emissions is not discussed.

Response: The discussion regarding the difference and its associated uncertainty is now in section 4 –'*The gas transfer velocity equation of W14 uses the square of the average neutral stability winds at 10 m height or second moment i.e., average of the quadratic windspeed. In this study, we used monthly average windspeed, i.e., the quadratic average windspeed for W14. The first method of calculation will estimate higher k values than the second one due to the averaging of the winds. We checked the differences between the two and found that the maximum difference is not more than 4.3 cm h^{-1} for June, July and August months and it is less than 2 cm h^{-1} for rest of the year, which does not contribute pointedly to the large uncertainty*.'.

2.1.7) L139-L145: What does "The flux due to σDMS" mean? Please also correct similar expressions as they are confusing.

Response: σ_{DMS} is calculated by calculating the standard deviation between H22, W20 and G18. This σ_{DMS} is used along with N00a parametrization, windspeed and SST data to get standard deviation in flux, which is shown in the monthly and annual σ_{DMS} plots (Fig. S10)." This standard deviation in calculated flux is the flux due to σ_{DMS}. The similar expressions are corrected for the other standard deviation parameters. This is now explained in the revised manuscript (L178 - L185).

2.1.8) The title of the manuscript is "Dimethyl sulfide (DMS) climatologies, fluxes, and trends – Part B: Sea-air fluxes", but no trend analysis is performed in this study. In L53, you mentioned that emission during 1948-2022 were used to calculate the DMS emission flux. However, no trend analysis is performed on the DMS emissions.

Response: Trend analysis is performed for DMS seawater concentration in Joge:Part A. An increasing trend of seawater DMS concentration is obtained, which also indicates that sea-air flux will increase. In this manuscript, Part B, the focus is on sea-air flux parametrization.

2.1.9) Introduction section: The author should add more on the sources and sinks of DMS in the ocean, and the chemical processes after it is released into the atmosphere. Then explain why DMS can affect climate.

Response: This information is now added in the introduction section (L25 - L35).

2.1.10) In addition to Table S1, a figure should be added in the main text to show the locations of the in-situ measurements used for DMS flux validation, with a legend showing two methods: eddy covariance and gradient flux technique.

Response: The suggested figure is added in the supplementary text as Figure S12. The text is also added in the data and methodology section (L70 - L72).

2.1.11) In Supplement, a figure should be added to show the locations of in-situ seawater measurements used to create the three seawater DMS climatologies (G18, W20, H22). This helps to determine in which regions the seawater concentrations in the climatology are more confident.

Response: This figure is available in part A of this manuscript.

References

1. *Blomquist, B. W., S. E. Brumer, C. W. Fairall, B. J. Huebert, C. J. Zappa, I. M. Brooks, M. Yang, et al. 2017. "Wind Speed and Sea State Dependencies of Air-Sea Gas Transfer: Results from the High Wind Speed Gas Exchange Study (HiWinGS)." Journal of Geophysical Research: Oceans 122 (10): 8034-8062.*

2. *Vettikkat, L., V. Sinha, S. Datta, A. Kumar, H. Hakkim, P. Yadav, and B. Sinha. 2020. "Significant emissions of dimethyl sulfide and monoterpenes by big-leaf mahogany trees: discovery of a missing dimethyl sulfide source to the atmospheric environment." Atmospheric Chemistry and Physics 20 (1): 375-389.*

3. *Wanninkhof, R. 2014. "Relationship between wind speed and gas exchange over the ocean revisited." Limnology and Oceanography Methods 12 (6): 351-362.*

4. *Yang, M., B. W. Blomquist, C. W. Fairall, S. D. Archer, and B. J. Huebert. 2011. "Air-sea exchange of dimethylsulfide in the Southern Ocean: Measurements from SO GasEx compared to temperate and tropical regions." Journal of Geophysical Research 116 (C4): c00f05.*

Response: All the above references are cited in the revised manuscript.

Response to Reviewer 3 comments for manuscript ID egusphere-2024-175. The comments are given in an italic typeface, and the responses are given in a bold typeface. The corresponding changes in the revised manuscript are highlighted in red.

3.1) This study led by D. Joge offers a valuable comparison of DMS flux parameterizations. Here are some additional thoughts to complement the two existing reviews.

In the introduction, it would be beneficial to clarify the distinctive contribution of this analysis. The authors briefly reference a previous intercomparison (lines 31–37) before delving into the specifics of their current work (lines 38–45). Inserting an intermediate paragraph summarizing the key differences between this study and prior research, along with the main outcomes from the companion paper (part A), would enhance the paper's coherence.

Response: The main outcomes of Part A are added to the introduction (L57- L59) and to the discussion section of the revised manuscript (L310 – L314).

3.2) Figures:

While the current version of the manuscript includes compelling figures, a few more could enhance reader comprehension. Here are some suggestions:

3.2.1) Section 2.1: Add figures to highlight the differences between the various parameterization methods (which may not be immediately clear from the equations alone). Potential figures could illustrate:

i) wind speed dependency of air-water gas transfer velocity for the different parameterizations, scaled to a Schmidt number at e.g., 20ºC;

ii) temperature dependency of air-water gas transfer velocity for the different parameterizations, scaled to different wind speeds (with one sub-figure per wind regime);

iii)temperature dependency of the Schmidt number for the different parameterizations.

Response: k vs u figures are added for all seven flux parametrizations in the supplementary text (Figs. S1 -S7), and the information related to these figures is added in the discussion section. The flux parametrization equations used in this study depend on the Schmidt number, which is a function of SST. The discussion related to this is added to this section (L316 - L320).

3.2.2) Section 3: While Figure 3 is commendable, Figures S3 and S4 could be more informative. A 'summary figure' combining results from these different figures could be beneficial. For instance, consider a figure where each grid box indicates the dominant contributing to the total uncertainty (using distinct colors for k, DMS, and wind). Alternatively, create one global map per parameter (k, DMS, wind) displaying, for each grid box, the percentage contribution to the total uncertainty.

Response: We tried to create a figure similar to the suggestion by the reviewer, but due to the coarse resolution of the data (1° x 1°), it was difficult to represent the information about uncertainty, especially in the monthly plots. Hence, we have not changed Figures S3 (now it is S10 in supplementary text) and S4 (now it is S11 in supplementary text) along with Figure 3. As the reviewer mentioned, the figures do show the needed information.

3.3) Additional comments:

3.3.1) Line 32: The statement "with the wind proven to be one of the most influencing factors" could be expanded upon. DMS flux measurements have revealed a decrease in gas transfer at medium to high wind speeds (> 10 m/s), attributed to wave-wind interactions and surfactant effects (Zavarsky et al., 2018), factors typically overlooked in traditional approaches (Bell et al., 2017). This discussion should be incorporated into the introduction.

Response: The text is now expanded with examples and citations (L43 - L45).

3.3.2) Line 43: A closing parenthesis is missing after W20.

Response: Parenthesis added (L56).

References

1. *Bell, T. G., Landwehr, S., Miller, S. D., de Bruyn, W. J., Callaghan, A. H., Scanlon, B., Ward, B., Yang, M., and Saltzman, E. S.: Estimation of bubble-mediated air–sea gas exchange from concurrent DMS and CO2 transfer velocities at intermediate–high wind speeds, Atmospheric Chem. Phys., 17, 9019–9033, https://doi.org/10.5194/acp-17-9019-2017, 2017.*

2. *Zavarsky, A., Goddijn-Murphy, L., Steinhoff, T., and Marandino, C. A.: Bubble-Mediated Gas Transfer and Gas Transfer Suppression of DMS and CO2, J. Geophys. Res. Atmospheres, 123, 6624–6647, https://doi.org/10.1029/2017JD028071, 2018*

Response: All the above references are cited in the revised manuscript.